

Determinant Monte Carlo for the Hubbard Model with Arbitrarily Gauged Auxiliary Fields

LIANG CHEN and A.-M.S. TREMBLAY
Département de physique et
Centre de recherche en physique du solide,
Université de Sherbrooke
Sherbrooke, Québec, Canada, J1K 2R1

ABSTRACT

Monte Carlo methods for the Hubbard model rely on a Hubbard-Stratonovich (HS) decomposition (auxiliary field method) to perform importance sampling on classical variables. Freedom in the choice of the local HS fields can be formally seen as a gauge choice. While the choice of gauge does not influence observable quantities, it may influence intermediate quantities in the calculation, such as the famous "fermion sign", and it may also influence the efficiency with which the algorithm explores phase space. The effect of arbitrary gauge choices on both aspects of the algorithm are investigated. It is found that in the single spin-flip determinantal approach, certain gauges lead to a better exploration of phase space. This improvement is demonstrated, in the intermediate coupling regime, by histograms which for the first time show the behavior expected from grand canonical simulations. It is also found that the improved phase space exploration can in practice offset the apparent disadvantage of a smaller fermion sign.

P.A.C.S. Numbers: 71.20.Ad, 71.10.+x, 74.65.+n

1. Introduction

Ever since Anderson's¹ seminal paper which followed the discovery of the cuprate superconductors² the Hubbard model has been the focus of much of the theoretical work on the subject.³ Numerical methods are playing a major role in this renewed intense activity on the Hubbard model because even though numerical approaches are restricted to small systems, they are in principle exact, while analytical methods are not completely reliable in the intermediate to strong coupling limit which is believed to be relevant for the oxide superconductors. Among the numerical methods, the so-called determinant Monte Carlo approach of Blankenbeller, Scalapino, Sugar and Hirsch⁴ has played a central role, producing a host of new

results^{5,6}, and also serving as benchmark for various analytical approximations⁷. In this Monte Carlo approach, as in many other approaches to interacting electrons, the Coulomb interactions are decoupled by the introduction of a Hubbard-Stratonovich (HS) field^{4,6,8}, allowing fermion degrees of freedom to be integrated out analytically to leave only classical HS variables in the simulation.

However there exists numerical difficulties in performing determinant Monte Carlo simulations: One which has been satisfactorily solved in the last two years⁹ is the stability problem associated with the low temperature limit. Of the two problems which remain, one is the well known "fermion sign problem", thoroughly discussed in Refs.¹⁰ and particularly in Refs.¹¹. The other problem is the so-called "sticking" problem at strong coupling which was recently studied in great detail in Ref.12.

In this paper we focus on the auxiliary field, or HS variables, to find out whether the arbitrariness in the choice of these variables can be used to alleviate the above-mentioned limitations. We have been stimulated by recent papers¹³ on the HS transformation which show that the choice of HS fields amounts to fixing a local gauge. It is easy to generalize this gauge formulation to the discrete HS transformation used in Monte Carlo simulations. In section II, we recall the Monte Carlo algorithm and the HS transformation. While the observable quantities are independent of the choice of gauge, intermediate quantities in the calculation can be gauge dependent. We explore in section III how non-trivial gauge choices can affect the fermion sign. For the gauges explored here we find that the fermion sign in the asymptotic low-temperature limit is not improved compared with the standard approach^{4,5,6} even though at higher temperature it is sometimes better. Concerning the other problem¹², sticking, it refers to difficulties of tunneling between thermodynamically allowed states. We show in section IV that a more symmetrical gauge choice can lead to clear improvements. In fact the improvement is so dramatic that in practical finite temperature calculations it can give shorter correlation times and offset the apparent disadvantage of having a smaller average fermion sign.

2. Gauge Freedom in Determinant Monte Carlo

Let us start with the single-band Hubbard Hamiltonian on a 2-d square lattice with nearest-neighbor hopping and on-site repulsion

$$\hat{H} = -t \sum_{\langle i,j \rangle, \sigma=1,2} (c_{i\sigma}^\dagger c_{j\sigma} + h.c.) - \mu \sum_{i,\sigma=1,2} n_{i\sigma} + U \sum_i (n_{i1} - \frac{1}{2})(n_{i1} - \frac{1}{2}). \quad (1)$$

As usual, one is interested in operator expectation values such as

$$\langle \hat{A} \rangle = \frac{\text{Tr} \hat{A} e^{-\beta \hat{H}}}{\text{Tr} e^{-\beta \hat{H}}} \quad (2)$$

where \hat{H} includes the chemical potential term μ since the calculation is in the grand-canonical ensemble. The trace over the fermion degrees of freedom cannot be performed analytically due to the quartic interaction term. In order to reduce the problem to a quadratic Hamiltonian, one first uses the Trotter formula to write the partition function in the form,

$$Z = \text{Tr} e^{-\beta \hat{H}} = \text{Tr} [e^{-\Delta\tau \hat{H}}]^L \approx \text{Tr} [e^{-\Delta\tau \hat{K}} e^{-\Delta\tau \hat{V}}]^L \quad (3)$$

where $\beta \equiv L\Delta\tau$, \hat{K} includes the quadratic pieces of \hat{H} (the hopping and chemical potential terms) while \hat{V} is the Coulomb repulsion term. The last expression above becomes an equality in the limit where L becomes infinite. It is useful to consider the Trotter product as describing evolution in imaginary time τ . Now that the quartic piece \hat{V} has been isolated, it can be made quadratic by using at every lattice point in space, i , and imaginary time, τ , the operator identity:

$$e^{-\Delta\tau U(n_{i,\tau} - \frac{1}{2})(n_{i,\tau} - \frac{1}{2})} = \frac{1}{2} e^{-\frac{U\Delta\tau}{4}} \sum_{z_i, \tau = \pm 1} e^{-\lambda z_i, \tau (2\vec{S}_{i,\tau} \cdot \vec{l}_{i,\tau})} \quad (4)$$

where $\cosh \lambda = \exp(U\Delta\tau/2)$, $\vec{S}_{i,\tau}$ is the spin operator with eigenvalues $\pm \frac{1}{2}$ and $\vec{l}_{i,\tau}$ is any three-dimensional unit vector. The discrete HS transformation introduced by Hirsch⁸ corresponds to the special case $\vec{l}_{i,\tau} \equiv \vec{e}_z$ in the above equation. (\vec{e}_z is a unit vector in the z direction). This special case amounts to a gauge choice for the HS variables since the vector field $\vec{l}_{i,\tau}$ can be chosen at will.¹⁴ The various gauges can be parametrized without redundancies by the set of directions in \mathbb{R}^3 , i.e. by elements of RP^2 , the unit sphere S^2 with antipodal points identified.

Returning to our main line of argument, the end result is that the partition function has been rewritten as

$$Z = \sum_{\{z_{i,\tau}\}} \text{Tr} \prod_i e^{-\Delta\tau \hat{K}} e^{-\Delta\tau \hat{V}'(i)} \quad (5)$$

where the fermion operators appear only quadratically in the transformed \hat{V}' . Note that while \hat{V}' is diagonal in space, imaginary time, and spin indices when $\vec{l}_{i,\tau} \equiv \vec{e}_z$, in the general case \hat{V}' has a block diagonal form with 2×2 matrices in spin space at every point of the space-time lattice. Continuing the calculation, we remark that the interacting fermions have been replaced by noninteracting fermions evolving in a field which depends on space, time and spin. The fermion trace can now be performed using standard techniques, and the result is

$$Z = \sum_{\{z_{i,\tau}\}} \det M(z_{i,\tau}) \quad (6)$$

where the matrix $M(z_{i,\tau})$ has dimension $2N \times 2N$ when there are N lattice sites in space. Had we chosen the "standard" HS transformation, the partition function would be written as the product of two determinants^{5,8} $\det M_1(z_{i,\tau}) \det M_2(z_{i,\tau})$ each with dimension $N \times N$.

Before closing this section, several remarks are in order. First, it should be obvious that a continuous instead of a discrete HS transformation would give results which are not qualitatively different⁸ from those discussed here. Second, note that in the case $U < 0$, one can generate an analogous gauge degree of freedom in the HS transformation⁸ by rotating¹⁴ fermion operators in Nambu space¹⁵ instead of spin space:

$$e^{\Delta\tau U(n_1 - \frac{1}{2})(n_1 - \frac{1}{2})} = \frac{1}{2} e^{-\frac{\Delta\tau U}{4}} \sum_{\vec{\tau}=\pm 1} e^{i\vec{\tau}\psi^\dagger(\vec{\sigma}\cdot\vec{\tau})\psi} \quad (7)$$

where ψ^\dagger is a row vector equal to $(c_1^\dagger \ c_1)$, $\vec{\sigma}$ are the Pauli matrices, $\vec{\tau}$ is any three-dimensional unit vector, as above, and $\cosh \lambda = \exp(|U|\Delta\tau/2)$. The usual treatment of the $U = -|U| < 0$ case (charge decoupling) corresponds to $\vec{\tau} \equiv \vec{e}_z$. Since in this case there is no sign problem, we do not consider it further in the present paper. In the $U > 0$ case however, it is interesting to notice that the anomalous decouplings introduced by Batrouni and Scalettar¹⁶ can be seen as a particular gauge choice in the corresponding Nambu space formulation of the $U > 0$ HS decoupling. More specifically, they took $\vec{\tau} = \vec{e}_y$ in the following equation,

$$e^{-\Delta\tau U(n_1 - \frac{1}{2})(n_1 - \frac{1}{2})} = \frac{1}{2} e^{\frac{\Delta\tau U}{4}} \sum_{\vec{\tau}=\pm 1} e^{i\vec{\tau}\psi^\dagger(\vec{\sigma}\cdot\vec{\tau})\psi} \quad (8)$$

with $\cos \gamma = \exp(-\Delta\tau U/2)$. The drawback of the above HS transformation is that its right-hand side becomes anti-Hermitian for each individual term in the sum, causing a sign problem even for the single-site case. Finally, more general HS transformations which interpolate between world-line and determinant Monte Carlo approaches have been proposed¹⁷, but since they generally give worse sign problems, we once again refrain from studying them here.

3. Gauge Dependence of the Fermion Determinant

One of the intermediate quantities which can be influenced by the gauge choice is the fermion determinant in Eq.(6). We remind the reader that for a Trotter decomposition with L time slices it takes the form,

$$\det(I + B_L B_{L-1} \dots B_1) \quad (9)$$

where each B_i is a $2N \times 2N$ matrix which is itself a product of a kinetic part which is diagonal in spin space; and a potential part which is diagonal in ordinary space but in general not in spin space. Recall that the absolute value of this quantity plays the role of the Boltzmann weight in the simulations. Given, however, that the determinant is independent of the choice of basis, it cannot depend on a change of gauge which corresponds to a global rotation of $\vec{\tau}_{i,\tau}$ over the whole space-time lattice. Indeed, such a change of gauge can be compensated by a canonical transformation (global rotation) on the fermion variables which leaves the Hamiltonian invariant.¹⁸

This gives us an easy way to check our code. We have verified that the determinant obtained with $\vec{l}_{i,r} = \vec{e}_x$ is identical with that obtained for $\vec{l}_{i,r} = \vec{e}_z$ for arbitrary configurations of the HS variables $x_{i,r}$.

Despite the fact then that the determinant has its own gauge group formed of global rotations, there is a very large set of local gauge choices for the auxiliary fields which influences the determinant, and hence its sign. It seems that in the wide class of gauges we tried, the standard one always corresponds to the best average sign in the asymptotic low temperature regime, even though this may not be the case at higher temperature. Although we cannot give a general proof of this, we can make it plausible by considering for example the half-filled case. In the standard gauge, $\vec{l}_{i,r} = \vec{e}_z$, the fermion sign is always positive. Indeed, in this gauge the fermion determinant is a product of up and down spin determinants and on bipartite lattices the sign of the determinant for up-spin electrons is identical to that for down-spin electrons^{4,6} due to the exact particle-hole symmetry. Suppose we take two points in the space-time lattice and make a rotation of $\vec{l}_{i,r}$ such that the x component of the spin operator

$$S_i^x = \frac{1}{2}(c_{i1}^\dagger c_{i1} + c_{i1}^\dagger c_{i1}) \quad (10)$$

now comes in the HS transformation at these two points. In the 'world-line' point of view⁶ of the standard gauge at half filling, for each exchange of up-spin electrons there is a corresponding exchange of down-spin electrons, but the existence of S_i^x at two points in the new gauge allows interchanges of spin-up electrons and spin-down electrons that cannot always be compensated: for example, at one point with a S_i^x , an up electron can become down, while at the other point with S_i^x a down can turn into up, leading to a final configuration with the same number of up and down electrons but with a net minus sign.

To test various gauge textures, we have chosen $\vec{l}_{i,r}$ in the plane spanned by \vec{e}_x and \vec{e}_z only. Indeed, components in the \vec{e}_y direction would force one to deal with complex matrices but, clearly, any gauge texture in the $z-y$ plane can be transformed to one in the $z-x$ plane by a global rotation which leaves the determinant unchanged. Hence, the only gauge textures we do not consider here are those where the three spin directions are involved. We do not see why these gauge textures would lead to results qualitatively different from those described below.

Note that the simulation is done with a single-spin-flip algorithm as usual, that is by sweeping through the space-time lattice of $x_{i,r}$ and doing the importance sampling with the ratio of fermion determinants before and after a single $x_{i,r}$ is flipped. The absolute value of the fermion determinant is used as a statistical weight while its sign is taken into account in the observables.

We consider five different gauges which can all be written in the general form,

$$\vec{l}_{i,r} = \sin(\theta_{i,r})\vec{e}_x + \cos(\theta_{i,r})\vec{e}_z \quad (11)$$

where $\theta_{i,\tau}$ is of the form,

$$\theta_{i,\tau} = \vec{k} \cdot \vec{r}_i - \omega\tau \quad (12)$$

with τ the time slice and \vec{r}_i the dimensionless position of the site in the two-dimensional plane containing $N_x \times N_y$ sites. We call the case $\vec{k} = (\frac{\pi}{N_x}, \frac{\pi}{N_y})$, $\omega = 0$ the spatially symmetrical gauge, the case $\vec{k} = (0, 0)$, $\omega = \frac{\pi}{t}$ the time symmetrical gauge, and the case $\vec{k} = (\frac{\pi}{N_x}, \frac{\pi}{N_y})$, $\omega = \frac{\pi}{t}$ the space and time symmetrical gauge. Two other gauges are studied: the random one, where $\theta_{i,\tau}$ takes uniformly distributed random values in the interval $[0, \pi]$, and the standard one where $\theta_{i,\tau} = 0$. Other even more 'wild' choices of gauges have been tried, none of which yielded good average signs.

Before quoting numerical results, we point out that in all cases one "measurement" is taken before each wrapping-up^{4,5,6} to the next time-slice and that no measurement is taken every other sweep through the space-time lattice. When we refer to warmup sweeps, one such sweep also corresponds to one complete update of the whole space-time lattice. Parameters for the simulations are given in units where t and Boltzmann's constant are unity.

Table 1 For the five different gauges discussed in the text: The average sign $\langle s \rangle$, the average number of up electrons $\langle N_\uparrow \rangle$ and down electrons $\langle N_\downarrow \rangle$, and the total energy in runs of 400 warmup sweeps and 50 000 measurements blocked by groups of 500 for a 4×4 system at half filling $\rho = 1$ with β and U in units where t and Boltzmann's constant are unity. $\Delta\tau$ is taken to be $\frac{1}{4}$ in all cases. For the time-symmetrical gauge, the space-time-symmetrical gauge, and the random gauge, the calculations are for $U = 4$ instead of $U = 8$ because in the latter case the average sign was too small.

Gauge	β	U	$\langle N_\uparrow \rangle$	$\langle N_\downarrow \rangle$	$\langle s \rangle$	E_{tot}/N
Space Sym.	4	8	7.94 ± 0.25	8.05 ± 0.25	0.47 ± 0.03	-0.56 ± 0.02
Time Sym.	4	4	7.93 ± 0.36	8.06 ± 0.36	0.46 ± 0.02	-0.84 ± 0.01
S-T Sym.	4	4	8.02 ± 0.77	7.98 ± 0.77	0.40 ± 0.02	-0.84 ± 0.03
Random	4	4	~	~	~ 0	~
Standard	4	8	7.85 ± 0.03	8.15 ± 0.03	1	-0.589 ± 0.004

Table 2 Same as Table 1 but for system 2×2 and a filling $\rho \sim 0.75$

Gauge	β	U	$\langle N_\uparrow \rangle$	$\langle N_\downarrow \rangle$	$\langle s \rangle$	E_{tot}/N
Space Sym.	4	8	1.49 ± 0.05	1.51 ± 0.04	0.46 ± 0.02	-1.47 ± 0.02
Time Sym.	4	8	1.48 ± 0.14	1.49 ± 0.13	0.42 ± 0.03	-1.49 ± 0.07
S-T Sym.	4	8	1.47 ± 0.22	1.49 ± 0.15	0.32 ± 0.03	-1.50 ± 0.07
Random	4	8	~	~	~ 0	~
Standard	4	8	1.48 ± 0.03	1.50 ± 0.03	0.59 ± 0.03	-1.48 ± 0.02

Some results for the average fermion sign $\langle s \rangle$ are summarized in Table 1 for half-filling, and Table 2 away from half-filling. Clearly, the standard gauge is the one which gives the best average sign $\langle s \rangle$. The other gauge which gives reasonable values of $\langle s \rangle$ is the spatially symmetrical gauge, $\vec{k} = (\frac{\pi}{N_x}, \frac{\pi}{N_y})$, $\omega = 0$, which we now study in more detail.

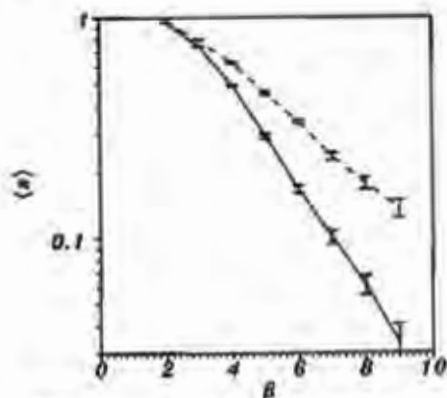


Figure 1: Average sign $\langle s \rangle$ of the fermion determinant against β for a 2×2 system at $U = 8$ with 3 electrons and $\Delta\tau = \frac{1}{8}$. We take 800 warmup sweeps and 800 000 measurements blocked by groups of 8 000. Solid line is for spatially symmetrical gauge and dashed line is for standard gauge. Both show the asymptotic exponential behavior. (For all numerical calculations, t and Boltzmann's constant are taken as unity.)

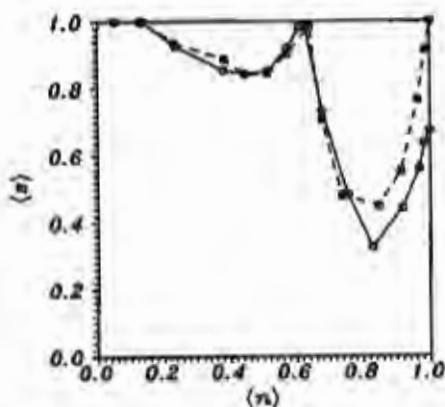


Figure 2: Average sign $\langle s \rangle$ of the fermion determinant as a function of band filling $\langle n \rangle$ for a 4×4 system at $U = 4$, $\beta = 4$ with $\Delta\tau = \frac{1}{8}$. We take 200 warmup sweeps and 200 000 measurements blocked by groups of 2 000. The solid line is for the spatially symmetrical gauge and the dashed line is for the standard gauge.

We have plotted in Fig. (1) the average sign in the standard gauge and in the spatially symmetrical gauge as a function of β for a 2×2 system with 3 electrons for $U = 8$ and $\Delta\tau = 1/8$. As one expects from previous simulations¹⁰ and from analytic calculations in the trial-wave-function approach¹¹, the average signs decrease exponentially as a function of β . Note however the different exponents and prefactors. Even though at $\beta = 2$ the average sign is actually better for the spatially symmetrical gauge, it is a prefactor effect. At sufficiently low temperature, the standard gauge gives better average sign. In Fig. (2) we have shown the average sign in the standard gauge and in the spatially symmetrical gauge as a function of band filling for a 4×4 system with $U = 4$, $\beta = 4$ and $\Delta\tau = 1/8$. One can see that both gauges have qualitatively the same dependence on filling but the spatially symmetrical gauge has an average sign consistently below that of the standard gauge.

4. Correlations and "Sticking" in Various Gauges

The "sticking" problem was thoroughly discussed recently in Ref.12. Briefly stated, the sticking problem is that as U and β increase, it becomes more and more difficult to produce statistically independent measurements (The configurations generated by the algorithm are more and more correlated). For example, suppose that at some low values of U and β we can obtain statistically independent results by grouping the measurements by blocks of 100 measurements. Then, at higher U and β , for fixed block size, we may find that there is a breaking of spin-flip symmetry $\langle N_{\uparrow} \rangle \neq \langle N_{\downarrow} \rangle$ which is outside the Monte-Carlo error bars! This is a clear manifestation of the fact that the measurements have become statistically correlated despite the fact that at smaller U they were grouped by big enough blocks that they were statistically uncorrelated. This comes from the fact that the Monte Carlo algorithm has difficulties to "tunnel" out of thermodynamically probable states to explore other equally probable ones. A way around this problem is suggested in Ref.12 where it is shown that global moves (flipping of HS fields at all time slices corresponding to a single site in ordinary space) improve the situation. Although sticking can be seen as a practical problem with the achievement of ergodicity, the algorithm is ergodic in the sense that in principle it can generate all of phase space. We refrain then from identifying sticking with ergodicity, although in practice they are related.

As a simple example of "sticking", consider in Table I the results for $\langle N_{\uparrow} \rangle$ and $\langle N_{\downarrow} \rangle$ at half filling for the standard gauge case. One observes that $\langle N_{\uparrow} \rangle$ and $\langle N_{\downarrow} \rangle$ differ by ten standard deviations. (Ref.¹² shows that at large U , $\langle N_{\uparrow} \rangle$ and $\langle N_{\downarrow} \rangle$ even stick to integer values, despite the fact that the calculation is grand-canonical.) By contrast, in the other gauges, Table I shows that $\langle N_{\uparrow} \rangle$ and $\langle N_{\downarrow} \rangle$ are always equal within Monte Carlo sampling errors. Choosing a less symmetrical gauge texture than the standard gauge then appears as a way to improve the efficiency with which phase space is explored within the single-spin-flip algorithm.

Another manifestation of the sticking problem which has been known for a long time⁶ is that much better statistics for the magnetic structure factor are obtained when one computes $\langle S^+ S^- \rangle$ instead of $\langle S^x S^x \rangle$. In other words, extremely long runs are needed to recover the rotational invariance of the original problem. This immediately suggests that another way to reduce the sticking problem is to use a gauge for the HS fields which is more rotationally symmetrical than the standard one. We also want to choose a gauge where the average fermion sign does not become too small. Guided by the discussion of the preceding section, we choose the spatially symmetrical gauge described below Eq.(12). To compare results obtained with this new gauge to results in the standard gauge, we display in Fig.(3) histograms for the distribution of spin-up electrons on a 4×4 system at half filling for both gauges. The histograms are obtained for $\beta = 4$ and $U = 4$. In the standard gauge it is very clear from Fig. (3a) that the system sticks to one up electron per site. The two large side peaks correspond to integer values of N_1 . By contrast, one can see from the histogram of Fig. (3b) that in our choice of gauge the "sticking" disappears. In fact, this is the first time that the histogram expected in grand-canonical simulations is observed in this regime. By contrast, the global moves in Ref.(12) forbid sticking to a single value of N_1 but the sticking still exists in the sense that N_1 and N_1 take "canonical" values¹², namely integer values.

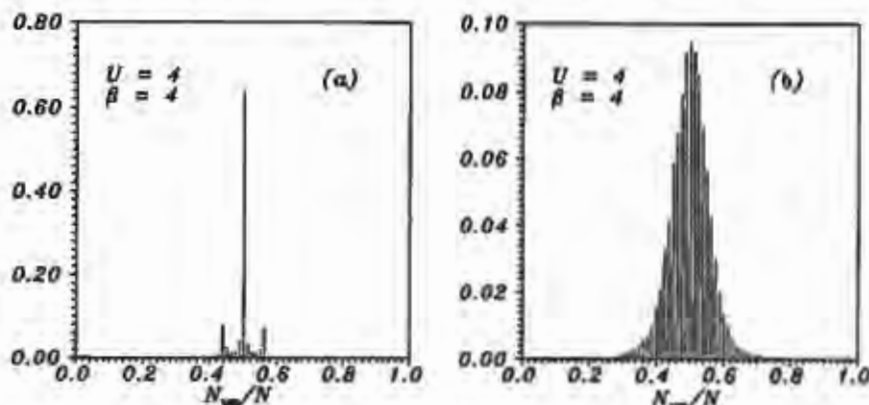


Figure 3: Typical normalized histograms of N_1/N for a 4×4 system at half filling with $\beta = 4$ and $U = 4$. In these runs, we take 400 warmup sweeps of the whole space-time lattice and 100 000 measurements blocked by groups of 1 for (a) and 5 for (b). (a) for the standard HS transformation (standard gauge) (b) for the spatially symmetrical gauge $\theta_{i,\tau} = (\vec{k} \cdot \vec{r}_i - \omega\tau)$, $\vec{k} = (\frac{\pi}{N_x}, \frac{\pi}{N_y})$, $\omega = 0$; $\Delta\tau$ is taken to be $\frac{1}{4}$ in all cases.

The improvement in the efficiency with which statistically independent regions of phase space are explored also manifests itself in the energy calculation. In fact the improvement is so dramatic that it can even offset the disadvantage of having a smaller sign. To illustrate this point, let us recall first that whatever the

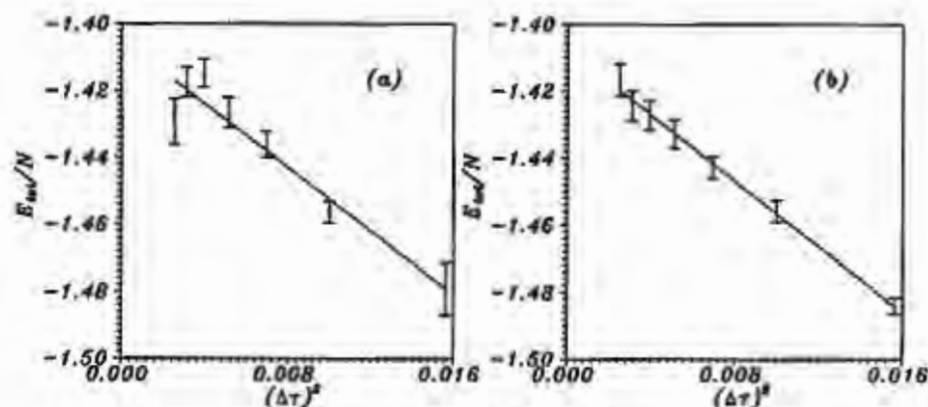


Figure 4: Energy per lattice site plotted as a function of the square of the imaginary time slice $\Delta\tau^2$ for a 2×2 system at $\beta = 4$, $U = 8$ and fixed chemical potential $\mu = 1.213$. The calculations are done with 1 000 000 measurements with block size of 10 000. Warmup sweeps varied from 800 to 2 000 as $\Delta\tau$ decreased. The solid lines are the best linear fit for the data. (a) for the standard HS transformation, (b) for the spatially symmetrical gauge. Clearly (b) gives a better extrapolation for the $\Delta\tau \rightarrow 0$, while (a) is less satisfactory due to sticking.

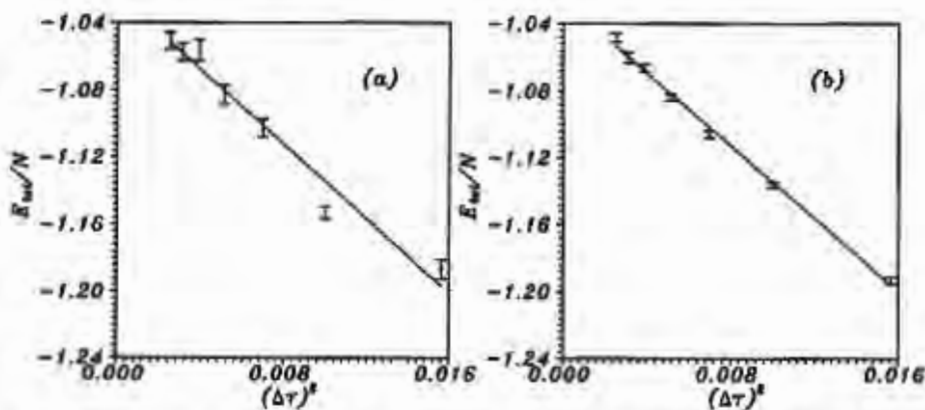


Figure 5: Energy per lattice site plotted as a function of the square of the imaginary time slice $\Delta\tau^2$ for a 2×2 system at $\beta = 4$, $U = 8$ and fixed chemical potential $\mu = 4$ corresponding to half-filling. The calculations are done with 1 000 000 measurements with block size of 10 000. Warmup sweeps varied from 800 to 2 000 as $\Delta\tau$ decreased. The solid lines are the best linear fit for the data. (a) for the standard HS transformation, (b) for the spatially symmetrical gauge. The average fermion sign $\langle s \rangle$ equals around 0.6 in the latter case, while it is unity in the former case. Despite its smaller average fermion sign, the spatially symmetric gauge (b) gives a better extrapolation for the $\Delta\tau \rightarrow 0$, while (a) is less satisfactory due to sticking.

value of the imaginary-time step $\Delta\tau$ in the Trotter decomposition, the results for the energy should be the same in any gauge. It is only the statistical accuracy obtainable at fixed number of measurements which can vary from one gauge to another. Figure (4a) shows the typical plot of energy versus $\Delta\tau^2$ which one would make to extrapolate the $\Delta\tau = 0$ value of the energy. The plot is for the standard HS gauge and all parameters are given in the caption. The plot is linear in $\Delta\tau^2$ as expected from the work of Fye and Suzuki¹⁰. However, one clearly sees some sticking at small $\Delta\tau^2$ since the energy seems to scatter around the straight line more than the error bars would suggest. By contrast, the results of Figure (4b), obtained for exactly the same parameters but in the spatially symmetrical gauge, show that in this case the Monte Carlo results are within error bars on the straight line. There is no sticking this time. It is quite remarkable that the results in the spatially symmetrical gauge are better than in the standard gauge, despite the fact that the average fermion sign is smaller in the new gauge than in the standard gauge (0.4 compared to 0.6). This striking result is even more dramatically illustrated by analogous results at half-filling where, despite the fact that in the standard gauge the sign is unity, the corresponding results for the energy (Figure 5a) are less statistically significant than those in the spatially symmetrical gauge (Fig. 5b) which has an average fermion sign of about 0.6.

We have also noticed that the spatially symmetrical gauge warms up to equilibrium in fewer sweeps than the standard gauge, confirming that the correlations between successive configurations are smaller in the new gauge than in the standard gauge. One should however note that in non-standard gauges, it takes more computer time to generate configurations because one works with B_i matrices of size $2N \times 2N$ instead of $N \times N$. Since the size of these matrices enters to the third power in the computing time, the algorithm for general gauges is at least 4 times slower than the standard one, (which computes up and down spins separately). Another factor slowing down the more general algorithm is the increased number of possible contractions in Wick's theorem and the more complicated aspect of the Sherman-Morrison and Woodbury formulas⁶ for updating Green's functions and determinant.

Finally, one should stress that it has to our knowledge never been seen before that simulations with an average fermion sign of 0.6 give more statistically significant results than simulations with an average sign of unity, as seems to be the case in Fig.(5). While detailed studies are still needed, we believe at this point that the statistical accuracy of the large sign case in usual simulations can be deceptive because of the extremely long correlation times of the sign and of other quantities in the standard gauge. We have several examples of this, but we briefly discuss two of them. First, compare in Table 1 the statistical accuracy of the space-symmetrical gauge and of the standard gauge. Given the value of $\langle N_1 \rangle - \langle N_1 \rangle$ it is clear that the statistical accuracy of the gauge with a smaller sign is closer to reality. It is only when the block size becomes of the order of the correlation time in the standard gauge that the advantage of the shorter correlation time of the new gauge shows up clearly on the actual error bars, as in Fig.(5). As a second example of the long

correlation times in the standard gauge, two consecutive runs of 10^6 measurements at $\Delta\tau = \frac{1}{20}$ in Fig.(4a) gave for the energy -1.394 ± 0.005 and -1.429 ± 0.007 . The two results are five standard deviations away from each other. The average fermion sign is 0.14 in the first case and 0.28 in the second, far from the expected 0.6 for this case.

5. Conclusion

In conclusion, we have explored the effect of arbitrarily gauged auxiliary fields on the fermion-sign problem and sticking problem which can occur in determinant Monte Carlo simulations of the Hubbard model. Within the wide class of gauges studied, the sign problem tends to become worse in the asymptotic low temperature limit, even though there is sometimes improvement at high temperature. However we have shown that in a gauge which is more symmetrical than the standard one, the single spin-flip algorithm explores phase space in a much more efficient way. In the intermediate coupling regime the sticking problem discussed in Ref.12 can be essentially eliminated: We were in fact able to obtain, for the first time, spin-up histograms which are the ones expected for such grand-canonical simulations. We have also shown total-energy calculations which illustrate that, at finite temperature and intermediate coupling, the smaller correlations between configurations generated in the new gauge can even offset the disadvantages coming from the smaller average fermion sign and lead to statistically more significant results than standard calculations.

6. Acknowledgments

We would like to thank the authors of Ref.12 for a preprint of their work and R. Scalettar for discussions. A.-M.S.T. would like to thank R.M. Fye for early conversations at the Institute for Theoretical Physics in Santa Barbara and S.Sorella for discussions at the I.C.T.P. in Trieste. The standard gauge code was written with the help of A. Reid, C. Boily and H. Néglise. We gratefully acknowledge the support of the Natural Sciences and Engineering Research Council of Canada (NSERC), the Fonds pour la Formation de Chercheurs et l'Aide à la Recherche (FCAR) of the Government of Québec and (A.-M.S.T.) the Canadian Institute for Advanced Research.

7. References

1. P.W. Anderson, *Science* **235** (1987) 1196.
2. J.G. Bednorz, K.A. Müller, *Z. Phys.* **B64** (1986) 189.

3. P.W. Anderson, and J.R. Schrieffer, *Physics Today* June (1991) p.55.
4. R. Blankenbecler, D.J. Scalapino, and R.L. Sugar, *Phys. Rev.* **D24** (1981) 2278; J.E. Hirsch, *Phys. Rev.* **B31** (1985) 4403.
5. See, for example, D.J. Scalapino, *High Temperature Superconductivity proceedings* (Published by Addison Wesley in 1990, edited by K.S. Bedell, D. Coffey, D.E. Meltzer, D. Pines and J.R. Schrieffer) pp. 314-367.
6. For a review, see for example E.Y. Loh, and J.E. Gubernatis, in *Electron Phase Transitions*, edited by W. Hauke and Y.V. Kopayev (North-Holland, New York, 1990).
7. Liang Chen, C. Bourbonnais, T. Li, and A.-M.S. Tremblay, *Phys. Rev. Lett.* **66** (1991) 369.
8. J.E. Hirsch, *Phys. Rev.* **B28** (1983) 4059.
9. G. Sugiyama and S.E. Koonin, *Ann. Phys.* **168** (1986); R.M. Fye and J.E. Hirsch, *Phys. Rev.* **B38** (1988) 433; S. Sorella, S. Baroni, R. Car, and M. Parrinello, *Europhys. Lett.* **8** (1989) 663; S.R. White, D.J. Scalapino, R.L. Sugar, E.Y. Loh, Jr., J.E. Gubernatis, and R.T. Scalettar, *Phys. Rev.* **B40** (1989) 506.
10. E.Y. Loh, Jr., J.E. Gubernatis, R.T. Scalettar, S.R. White, D.J. Scalapino and R.L. Sugar, *Phys. Rev.* **B41** (1990) 9301; S.B. Fahy, and D.R. Hamann, *Phys. Rev. Lett.* **65** (1990) 3437; D.R. Hamann, and S.B. Fahy, *Phys. Rev.* **B41** (1990) 11 352.
11. Sandro Sorella, *Int. J. Mod. Phys.* **B5** (1991) 937; S. Fahy, and D.R. Hamann, *Phys. Rev.* **B43** (1991) 765.
12. R.T. Scalettar, R.M. Noack and R.R.P. Singh, *Phys. Rev. B* (in press).
13. H.J. Schulz, *Phys. Rev. Lett.* **65** (1990) 2462; Z.Y. Weng, C.S. Ting and T.K. Lee, *Phys. Rev.* **B43** (1991) 3790.
14. The left-hand side of Eq.(4) is invariant under $SU(2)$ transformations of the fermion creation-annihilation operators. In other words, this part of the Hamiltonian is invariant under the choice of quantization axis. It is this symmetry which reflects itself on the HS fields on the right-hand side of Eq.(4). This freedom in the choice of quantization axis can be kept in the kinetic energy term as well, but only if a gauge field is introduced, as in Refs.¹³.
15. The left-hand side of Eq.(7) (see also ¹⁴), is invariant under $SU(2)$ transformations but this time in pseudo-spin space. This "hidden symmetry" of the Hubbard Hamiltonian and the associated conserved quantity was recently studied by C.N. Yang, and S.C. Zhang, *Mod. Phys. Lett.* **B4** (1990) 759; Souheng

Zhang, *Int. J. Mod. Phys.* **5** (1991) 153. In these papers, the symmetry is studied as a global symmetry of the full Hubbard Hamiltonian. Combined with rotational invariance, one has overall a $SO(4) = SU(2) \times SU(2)/Z_2$ symmetry. This global symmetry, which is also a local symmetry of the interaction part of the Hamiltonian, can be promoted to a local symmetry of the full Hamiltonian if the appropriate gauge fields are introduced in the kinetic energy operator, as in Refs.¹³. See also I. Affleck, Z. Zou, T. Hsu, and P.W. Anderson, *Phys. Rev.* **B38** (1988) 745.

16. Ghassan George Batrouni and Richard T. Scalettar, *Phys. Rev.* **B42** (1990) 2282.
17. J.E. Hirsch, *Phys. Rev.* **B34** (1986) 3216.
18. The equality between the weights generated by apparently different HS transformations in the work of Batrouni and Scalettar¹⁶ can be explained by the fact that the different HS transformations are in fact related by global rotations in Nambu space, as formulated in Eq.(8), and hence they are related by a canonical transformation.
19. R.M. Fye, *Phys. Rev.* **B33** (1986) 6271; M. Suzuki, *Phys. Lett.* **113A** (1985) 299.